Carbohydrate Polymers 88 (2012) 1149–1156

Contents lists available at SciVerse ScienceDirect

Carbohydrate Polymers

journal homepage: www.elsevier.com/locate/carbpol

Structural features and changes of lignocellulosic biomass during thermochemical pretreatments: A synchrotron X-ray scattering study on photoperiod-sensitive sorghum

Feng Xu[a], Yong-Cheng Shi[b,*], Donghai Wang[a,*,1]

[a] Department of Biological and Agricultural Engineering, Kansas State University, KS 66506, United States
[b] Department of Grain Science and Industry, Kansas State University, KS 66506 United States

ARTICLE INFO

Article history:
Received 8 October 2011
Received in revised form 2 January 2012
Accepted 14 January 2012
Available online 2 February 2012

Keywords:
Biomass structure
WAXD
SAXS
Cellulose
Pretreatment

ABSTRACT

Fundamental understanding of the structural changes during pretreatment of lignocellulosic biomass could lead to improved processes and cost reductions for bioethanol production. Synchrotron wide-angle X-ray diffraction (WAXD) and small-angle X-ray scattering (SAXS) were used to study the structures of different parts of photoperiod-sensitive sorghum and structural changes during various pretreatments. WAXD study showed that the PS sorghum rind had oriented crystal peaks and the highest degree of crystallinity, whereas the crystalline structures of the inner pith and leaf were less ordered. Orientation distribution of cellulose changed during pretreatments. Crystalline cellulose was degraded partially by acid pretreatment and a smooth pore-boundary surface structure of cellulose was noted by SAXS. Alkali pretreatment transformed part of the cellulose to a more stable form and increased the crystal size of cellulose. The study provides information on a large length scale to understand how structure changes with different pretreatments.

1. Introduction

Lignocellulosic biomass has become an important source for production of bioethanol and other products (Mielenz, 2001). Photoperiod-sensitive (PS) sorghum, with the advantages of high biomass yield and drought tolerance, can be grown in semiarid areas that are too dry for corn growth (Alagarswamy, Reddy, & Swaminathan, 1998; Clerget, Dingkuhn, Goze, Rattunde, & Ney, 2008; Rosenow, Quisenberry, Wendt, & Clark, 1983). The low lignin content in PS sorghum makes it competitive for biofuel production (Xu et al., 2011).

Pretreatment, including physical size reduction and chemical reaction, is important for cellulosic ethanol production because, unlike starch-ethanol production, cellulose in biomass is usually embedded in a network structure (Rubin, 2008). Lignin, one of the amorphous components, acts as a cellulase absorber during enzymatic hydrolysis (Berlin et al., 2005; Hidaka, Takizawa, Fujikawa, Ohneda, & Fukuzumi, 1984), which significantly increases processing cost and makes biomass conversion less effective. A successful pretreatment would maximize all available biomass components for economical processing. Different pretreatment strategies have been proposed for biomass processing, some of which have proven effective (Mosier, Hendrickson, Ho, Sedlak, & Ladisch, 2005; Mosier, Wyman, et al., 2005); however, profitable commercialization of cellulose-ethanol production is still lacking. Knowing the detailed structural features of lignocellulosic biomass and the structural changes during pretreatment would help develop effective ways to reduce pretreatment costs.

Until now, the effects of pretreatment on changes at the molecular level have not been fully understood. Wide-angle X-ray diffraction (WAXD) has been used for a long time in studying the crystalline structure of cellulose (Nishiyama, Langan, & Chanzy, 2002) and has been used frequently for the study of crystalline structure in biomass processing (Oh et al., 2005). For samples with crystal orientation, such as natural cellulose in biomass, crystals generate certain aligned arcs in a 2D WAXD pattern, which provides much more information about 3D structure order (Burger, Hsiao, & Chu, 2010). Previous X-ray studies on biomass focused primarily on powder diffraction, and no detailed study is available on orientation discrepancy as well as orientation changes during biomass processing. Small-angle scattering techniques, including small-angle neutron scattering (SANS) and small-angle X-ray scattering (SAXS), are able to probe structures over a size ranging from approximately 1 nm to several hundred nanometers, larger than those found with WAXD, and have been applied to the study of synthetic and natural polymers (Blazek & Gilbert, 2011; Chu & Hsiao,

* Corresponding authors. Tel.: +1 785 532 6771; fax: +1 785 532 7010.
E-mail addresses: fxu@ksu.edu (F. Xu), ycshi@ksu.edu (Y.-C. Shi), dwang@ksu.edu (D. Wang).
[1] Tel.: +1 785 532 2919; fax: +1 785 532 5825.

0144-8617/$ – see front matter © 2012 Elsevier Ltd. All rights reserved.
doi:10.1016/j.carbpol.2012.01.041

2001). However, only limited SAXS studies have been reported on biomass structure (Lichtenegger, Reiterer, Stanzl-Tschegg, & Fratzl, 1999). Recently, SANS has been used to study cellulose extract from switchgrass (Pingali et al., 2010a) and cell wall nanostructure in dilute acid pretreated biomass (Pingali et al., 2010b). The diameter of cellulose fibrils was reported to be 2.5 nm in sprucewood (*Picea abies*) through SAXS study (Jakob, Fratzl, & Tschegg, 1994). In addition, SAXS has been used to study individual components including cellulose and lignin (Astley & Donald, 2001; Canetti, Bertini, De Chirico, & Audisio, 2006; Nishiyama et al., 2002; Vickers, Briggs, Ibbett, Payne, & Smith, 2001). Therefore, SAXS could be a useful tool to study the effects of different pretreatments on biomass structure. Synchrotron radiation, with the benefits of a high ratio of signal to noise and high intensity, has been employed in a number of studies (Yu et al., 2003). The small beam divergence of incident X-ray and the high-energy source of synchrotron X-ray enable the performance of advanced experiments. The synchrotron X-ray allows completing data collection in less than one minute, making possible real-time monitoring of structural changes.

In this study, we used a combination of WAXD and SAXS to reveal the structure of lignocellulosic biomass, including multiple components in both crystalline and amorphous state. Instead of ground powder, we used biomass chips, making it possible to reveal crystal orientation distribution changes and their effects on subsequent biomass processing. For the first time, the structure of different parts of PS sorghum and structural changes during pretreatments were studied by both WAXD and SAXS. The objectives of this study were to understand the structural differences of the parts of PS sorghum, and to study how their structures change during pretreatments at a molecular level using WAXD and SAXS.

2. Materials and methods

2.1. Materials

The PS sorghum was harvested at physiological maturity from Riley County, Kansas. Different parts of the biomass, including rind, pith, and leaf, were obtained from three strains for comparison and prepared by knife-cutting and air-drying in an oven at 50 °C for 12 h. A detailed explanation of the three biomass parts is depicted in Fig. 1. The samples of PS rind and pith were cut from PS stalk between internodes. All chemicals used in this research were of analytical grade and purchased from Sigma–Aldrich, Inc. (St. Louis, MO, USA).

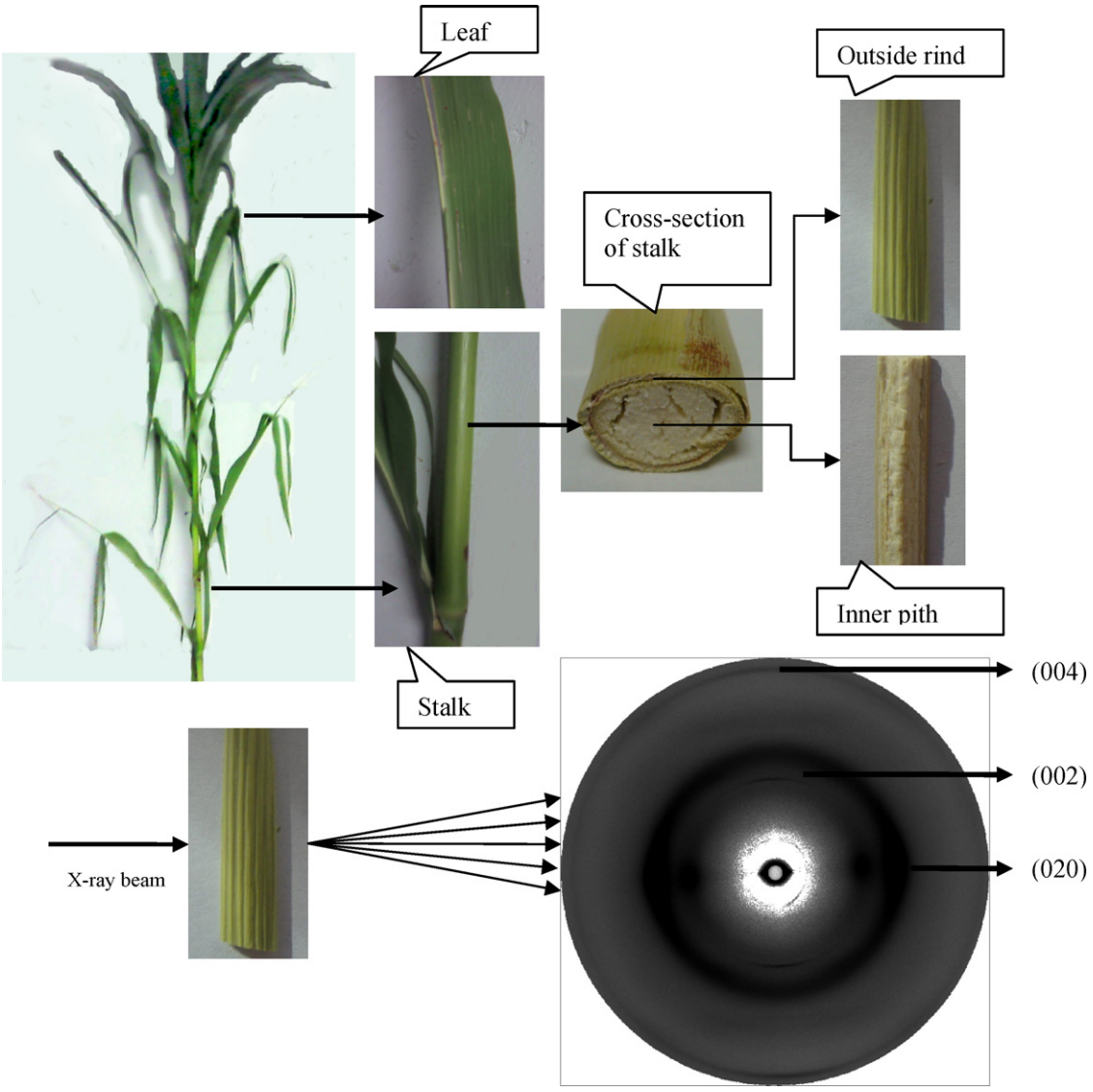

Fig. 1. Illustration of photoperiod-sensitive sorghum in different parts and a typical 2D WAXD pattern of rind.

2.2. Pretreatments

Pretreatment of biomass was conducted under different conditions (Silverstein, Chen, Sharma-Shivappa, Boyette, & Osborne, 2007). A small piece of chip, with a surface dimension of 0.5 × 2 cm, was loaded into 10 ml chemical solution for pretreatment. For acid pretreatment, a chip sample was loaded into a pressure tube (No. 8648, Ace Glass Inc., Vineland, NJ, USA) containing 2% (w/w) sulfuric acid solution, the temperature was increased to 120 °C, and the solution was held at this temperature for 1 h. For alkali pretreatment, a chip sample was loaded into a pressure tube containing 1% (w/w) of sodium hydroxide and the temperature was maintained at 90 °C for 2 h. For ammonia pretreatment, a chip sample was loaded into a pressure tube containing 10% (v/v) ammonia solution and the temperature was then maintained at 90 °C for 2 h. All the pretreatment experiments were done in triplicate. After pretreatment, the solid samples were air-dried (~8% moisture content) for X-ray testing, and the solutions were subjected to reducing sugar analysis with high performance liquid chromatography, as previously reported (Xu et al., 2011). In addition, the biomass chips were determined for mass loss after pretreatments.

2.3. Synchrotron WAXD and SAXS

WAXD and SAXS experiments were carried out at the advanced polymers beamline (X27C), National Synchrotron Light Source, Brookhaven National Laboratory, in Upton, NY. Details of the experimental setup at the X27C beamline have been reported elsewhere (Chu & Hsiao, 2001). The wavelength used was 0.13714 nm. The sample-to-detector distance was 129.3 mm for WAXD and 1789.3 mm for SAXS, respectively. A 2D MAR-CCD (MAR USA, Inc.) X-ray detector was used for data collection. For X-ray study of chips, the direction of the X-ray is perpendicular to fiber direction. Three locations along fiber direction in each chip were used for measurement.

2.4. Data processing

Two dimensional WAXD patterns were first corrected with air background, then performed with Fraser correction using Polar software (Precision Works, NY) (Ran, Wang, Burger, Chu, & Hsiao, 2002). The orientation of cellulose was analyzed from the 2D corrected pattern, and crystallinity and crystal size were estimated from the integrated 1D diffraction intensity profile. Crystallinity (mass crystallinity if not specified, percentage of crystalline cellulose in biomass) was estimated from an integrated diffraction intensity profile as the ratio of the total crystal peak diffraction intensity to the total diffraction intensity. A peak-fitting process was employed with Igor Pro 6.20 (WaveMetrics Inc. Lake Oswego, OR). The monoclinic crystal system was assumed to be the crystal unit of cellulose I_β (Heiner & Teleman, 1997). Crystal size along and perpendicular (an axis of unit cell) to the fiber direction (*c*-axis) were estimated from planes (0 0 4) and (0 2 0), respectively (Eq. (1)). Since the Bragg reflection may be broadened by both crystallites with finite size and possible imperfections in crystal lattice, the equation here could be used only as a lower bound estimation of crystal size.

$$L_{w(h\ k\ l)} = \frac{K\lambda}{\mathrm{FWHM}_{2\theta}\cos\theta} \tag{1}$$

where θ is the Bragg angle corresponding to the plane, K is the constant of 0.9 for cellulose (Alexander, 1954), λ is the wavelength, and $\mathrm{FWHM}_{2\theta}$ is the full width at half maximum of the reflection in the radial direction.

For crystal orientation analysis, it was assumed that the cellulose in biomass is cylindrically symmetrical similar to a fiber-like system. Thus, the orientation parameter could be calculated with plane (0 2 0) as described elsewhere (Burger et al., 2010). The Hermans' orientation parameter $\bar{P}_2$ varies from 0 for completely isotropic systems to 1 for perfectly oriented systems.

Two-dimensional SAXS data was first corrected with air background, then integrated into 1D intensity data. The 1D data was analyzed using Igor Pro 6.20 with the Irena package. The unified equation was used for analysis of SAXS data (Beaucage, 1995). The equation defines multiple levels, and each level may contain Guinier region describing an average structural size and power-law region describing the mass or surface fractal. The unified model is given by:

$$I(q) = G_i \exp\left(\frac{-q^2R_{gi}^2}{3}\right) + B_i \exp\left(\frac{-q^2R_{g(i-1)}^2}{3}\right) \times \left\{\frac{[\mathrm{erf}(qR_{gi}/6^{1/2})]^3}{q}\right\}^{P_i} \tag{2}$$

where i represents the structural levels; G_i is the exponential prefactor; R_{gi} is the radius of gyration; B_i is a constant prefactor specific to the type of power-law scattering, P_i; and the magnitude of the scattering vector is defined as $q = 4\pi \sin\theta/\lambda$ (θ is half of the scattering angle).

3. Results and discussion

3.1. Structure features in different parts

3.1.1. WAXD study

A typical 2D WAXD pattern of lignocellulosic biomass is shown with indexed peaks (Fig. 1). We compared the samples from three strains of PS sorghum and found that the crystalline structure of the different strains were identical. Three parts of PS sorghum (rind, pith, and leaf) were chosen as objects in this research. The crystal of the PS sorghum rind contained a significant oriented portion (0 2 0 plane) that was not observed in the other patterns (Fig. 2) because they were isotropic. Note that the reflections here were indexed (Fig. 1) according to the monoclinic two-chain unit cell (Gardner & Blackwell, 1974). The oriented pattern showed the features of native cellulose (I) in the plant as previously reported (Jakob, Fengel, Tschegg, & Fratzl, 1995; Konnerth, Gierlinger, Keckes, & Gindl, 2009; Nishiyama et al., 2002). The Hermans' orientation factor was then calculated as shown in Table 1. Generally, the orientation factor for a perfectly oriented system is 1. In this case, the factor of the PS sorghum rind is 0.26, indicating that the natural cellulose in the rind has oriented structure, whereas the cellulose structure in sorghum pith and leaf was isotropic with factors close to zero. The oriented pattern was only observed from the PS sorghum rind, suggesting that the structural order of cellulose in different parts of PS sorghum is different. Crystal orientation was reported to be related to the mechanical properties of polymer (Britton, Liang, Dunne, & Wilkinson, 2010; Gurarie, Otsuka, Jamieson, Williams, & Conway, 2002), but it is not yet clear how the mechanical properties of certain biomass is correlated to the orientation characteristics

Table 1
Crystallinity, crystal size, and orientation factor of photoperiod-sensitive sorghum in different parts estimated from the WAXD.

	Crystallinity (%)	Crystal size (0 2 0) (nm)	Hermans' orientation factor $\bar{P}_2$
Rind	29	2.49	0.26
Pith	24	2.45	0.08
Leaf	10	2.62	0.06

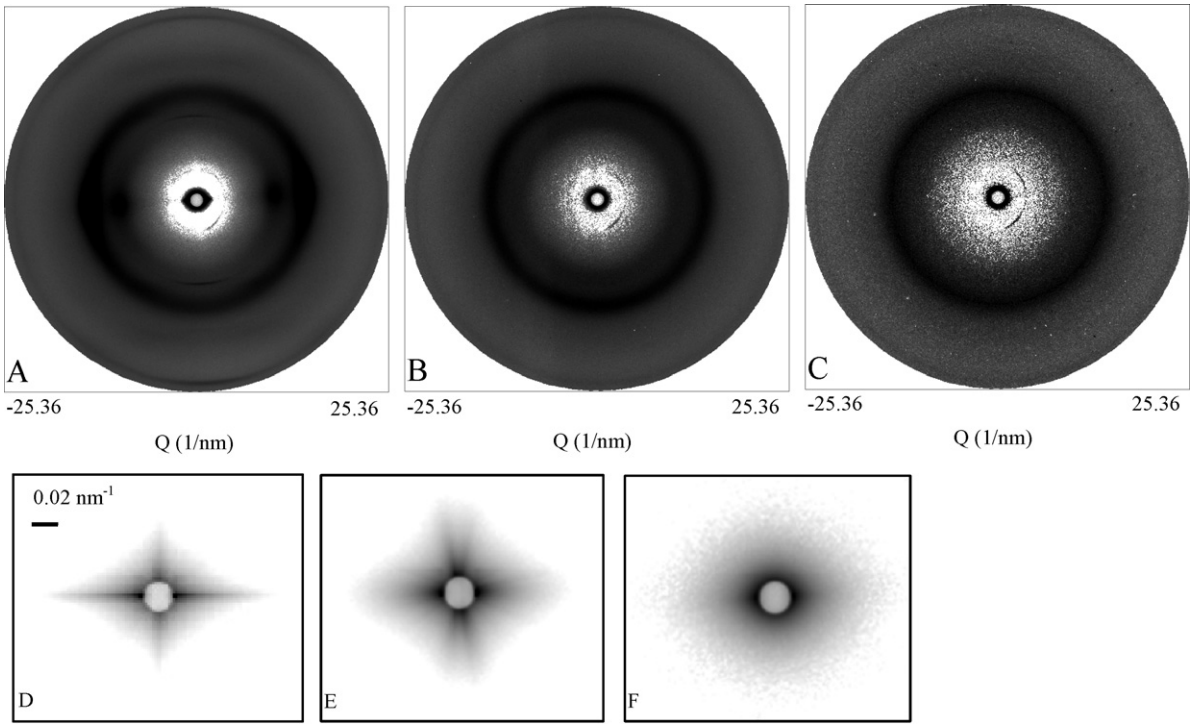

Fig. 2. WAXD and SAXS patterns of photoperiod-sensitive sorghum in different parts (WAXD, A: outside rind; B: inner pith; C: leaf; SAXS, D: outside rind; E: inner pith; F: leaf).

of cellulose. The difference in cellulose assembly between the different plant parts may influence the downstream processing of biomass conversion such as enzymatic hydrolysis. Study of the effects of the preferred orientation on processing is suggested for improving processing efficiency and for development of plant breeding strategies. Compared with the strong crystalline pattern of PS sorghum pith, the diffraction circle of the leaf is diffused, indicating an increased amount of amorphous components in the leaf, as confirmed by the crystallinity study below.

One-dimensional profiles were then obtained by integrating the corrected 2D pattern. Notably, for the oriented pattern, the integration of the 2D pattern without Fraser correction would result in significant deviation (Ran et al., 2002). Different crystal peaks were deconvoluted from the diffraction plot with a peak-fitting process. Crystallinity and crystal size were then calculated (Table 1). The PS sorghum rind had the highest crystallinity (29%) among those samples, whereas the leaf had a low crystallinity (10%). Crystallinity is considered an important index related to mechanical properties (Gassan & Bledzki, 1999), and a high crystallinity could be one of the reasons for increasing the cost of size reduction. Different parts of PS sorghum exhibited no significant difference in crystal size (plane 0 2 0) (Table 1). Similar results were also reported about the crystal size (plane 0 2 0) of lemon and maize cellulose (Rondeau-Mouro et al., 2003). Since other factors may broaden the peak that was used for crystal size estimation, such as internal lattice defects, the estimates here are minimal.

3.1.2. SAXS study

SAXS study of biomass parts is reported here for the first time. The 2D SAXS patterns of different parts of PS sorghum were significantly different (Fig. 2). Anisotropic patterns were found with both rind and pith parts, indicating oriented structure of biomass on this length scale (Jungnikl, Paris, Fratzl, & Burgert, 2008). For PS sorghum rind, both equatorial streak and meridional streak were shown on the SAXS 2D pattern (Fig. 2D). The elongated shape of the equatorial streak indicated that microvoids were needle-shaped and aligned parallel to the fiber direction (Chen et al., 2007). The meridional scattering suggested that periodic lamellar structure existed between the crystalline and amorphous regions (Chen et al., 2007). It is possible that there are two directions of microvoids in pith that are vertical to each other. For PS sorghum pith, the meridional streak, unlike the equatorial streak, was found to be splitting. The similar split pattern in equatorial direction was also reported in SAXS pattern of latewood as a result of the existence of microfibril angle (Jakob et al., 1994; Lichtenegger et al., 1999), suggesting that tilted microvoids are perpendicular to the *c*-axis (fiber direction). The evidence here, however, is not sufficient to support the particular structure of PS pith. Complementary structure technologies are needed for further investigation. The periodic interval along the microfibrils, which could be estimated from the position of the maximum scattering in the meridional direction (Chen et al., 2006), was about 178 nm for the PS sorghum rind. This value was close to a microfibrils periodic interval of 150 nm for ramie cellulose (Nishiyama et al., 2003). In this study, the PS sorghum rind did not give any peak corresponding to 6–7 nm repeat reported on flax (Astley & Donald, 2001). For PS sorghum leaf, no significant streak in either direction was observed. The diffused SAXS leaf pattern, together with the WAXD pattern, suggested that the structure of the leaf was less ordered.

One-dimensional SAXS profile was then obtained by integrating 2D patterns for analysis, and the P values in the power-law region of the different parts were calculated to be in the range of 3.5–4.0, indicating that the materials are surface fractals (Koberstein, Morra, & Stein, 1980; Schmidt, 1991).

3.2. Effects of pretreatments on PS rind

3.2.1. WAXD study

The effects of different pretreatments on the structure of PS sorghum rind were studied to reveal how chemicals changed the biomass structure at a molecular level, such as cellulose structure in orientation distribution and crystalline characteristics. With the

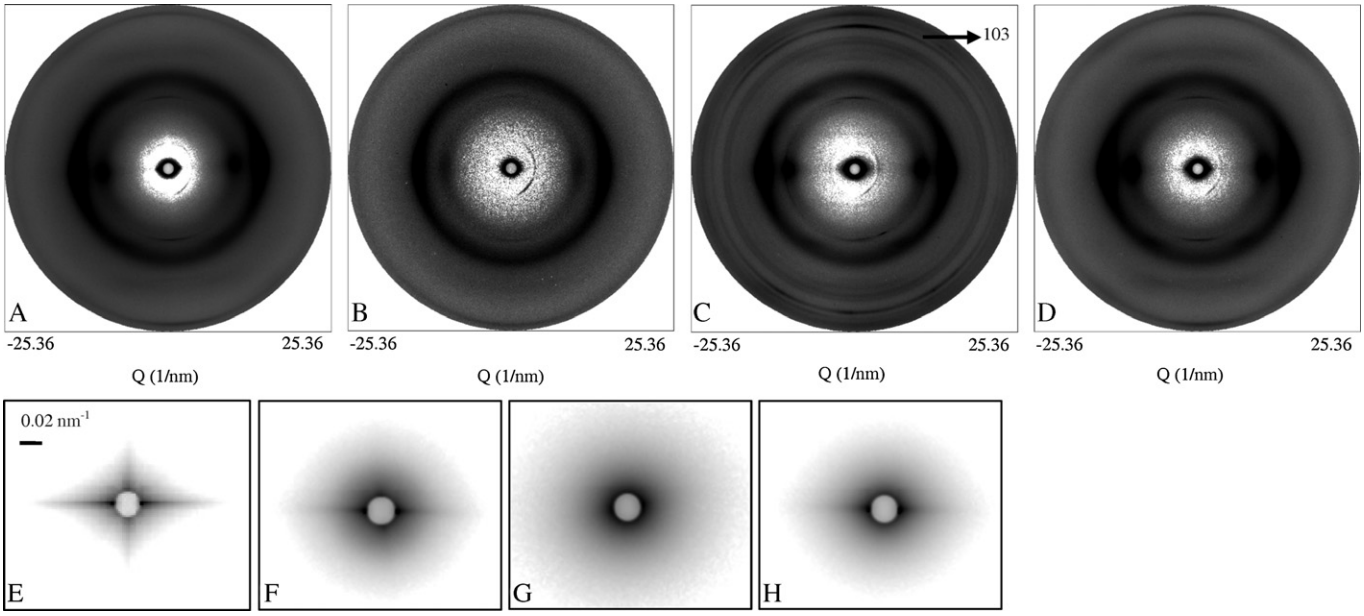

Fig. 3. WAXD and SAXS patterns of photoperiod-sensitive sorghum with different pretreatments (WAXD, A: untreated; B: acid treated; C: alkali treated; D: ammonia treated; SAXS, E: untreated; F: acid treated; G: alkali treated; H: ammonia treated).

acid pretreatment, the 2D pattern changed (Fig. 3) and the orientation factor (P_2) decreased (Table 2), indicating that the spatially ordered cellulose was distorted. However, the orientation factor increased with both the alkali and ammonia pretreatment. With the alkali pretreatment, new crystal peaks were found at 2θ angle of 26.7°and 28.7° in the 1D plot (corresponding to the circles in the 2D pattern of Fig. 3C), which are the diffraction of chemicals (e.g., Na_2CO_3) during the alkali pretreatment (Gancy, 1963). A new oriented pattern (plane 1 0 3) was found, that was not shown in the WAXD pattern of cellulose I (Fig. 3A and C) and was reported in the WAXD pattern of cellulose II (Chen et al., 2007). The new oriented peak is one reason why the orientation factor increased; however, the alkali treatment conditions used in this study were too mild to completely convert cellulose I in the PS sorghum rind to cellulose II, which is a more stable form with antiparallel chain structure in NaOH solution (Aravindanath, Iyer, & Sreenivasan, 1986; Kolpak & Blackwell, 1976). For biomass system, the removal of lignin by the alkali pretreatment could result in an increase in the accessible area of cellulose and a decrease in the amount of cellulase absorbed on lignin, which is favored for improving the efficiency of enzymatic hydrolysis. The partial transition of cellulose to a stable form, however, could increase the resistance of cellulose to cellulase reaction. Notably, the transition of cellulose usually takes place with the change of cellulose crystallinity (percentage of crystalline cellulose in cellulose), which is another factor affecting enzymatic hydrolysis. Thus, the extent of enzymatic hydrolysis is affected by multiple factors.

Crystallinity increased after all the pretreatments. Since a significant mass loss (about 30%) was found after the acid pretreatment and both glucose and xylose were detected in the solution (data not shown), the increase in crystallinity could be a result of the removal of amorphous parts, including hemicellulose and amorphous cellulose. Considering that the crystallinity increased only 4% and the mass loss was about 30%, we believe that part of the crystalline cellulose was hydrolyzed by acid and crystalline structure might have changed, which could be related to the decrease in orientation factor. More detail will be discussed in Section 3.2.2. Lignin extraction by NaOH is one of the reasons for increased crystallinity with the alkali pretreatment. In addition, recrystallization was reported to take place during the mercerization (Hermans, Vermaas, & Weidinger, 1950; Kroon-Batenburg, Bouma, & Kroon, 1996). For the ammonia pretreatment, depolymerization of lignin, which resulted in lignin removal from biomass to solution (Balan et al., 2009), could be one cause of an increase in crystallinity (Mosier, Hendrickson, et al., 2005; Mosier, Wyman, et al., 2005).

The 2D WAXD patterns showed that the alkali pretreatment changed the crystalline structure significantly. Compared with the untreated sample, the crystal sizes of cellulose in both planes (0 2 0) and (0 0 4) increased significantly (Table 2). This could be explained by the aggregation of cellulose in NaOH solution. An increased temperature (90 °C, in this case) favored cellulose aggregation (Roy, Budtova, & Navard, 2003). The effect of crystal size on enzymatic hydrolysis is not yet known, but the aggregation of cellulose could decrease the accessible surface area of cellulose. Therefore, as discussed in cellulose transition, the structural change of cellulose itself by the alkali pretreatment might not be helpful for enzymatic hydrolysis.

Table 2
Crystallinity, crystal size, and orientation factor of photoperiod-sensitive sorghum with different pretreatments.

	Crystallinity (%)	Crystal size (nm)		Hermans' orientation factor $\bar{P}_2$
		(0 2 0)	(0 0 4)	
Untreated	29	2.49	2.75	0.26
Acid treated	32	2.52	2.74	0.21
Alkali treated	32	2.86	3.13	0.32
Ammonia treated	39	2.47	2.64	0.33

3.2.2. SAXS study

After the ammonia pretreatment, the elongated shape in the equatorial direction was reduced (Fig. 3), indicating that microvoids were reduced during the pretreatments. The elongated shape almost disappeared after the alkali pretreatment, indicating a decrease in orientation and length of microvoids (Crawshaw, Bras, Mant, & Cameron, 2002). Since sodium hydroxide could effectively dissolve lignin and partially remove hemicellulose (Silverstein et al., 2007), the shortening or disappearance of microvoids could be a result of significant structure disruption with the alkali pretreatment. In addition, the drying process may cause irreversible

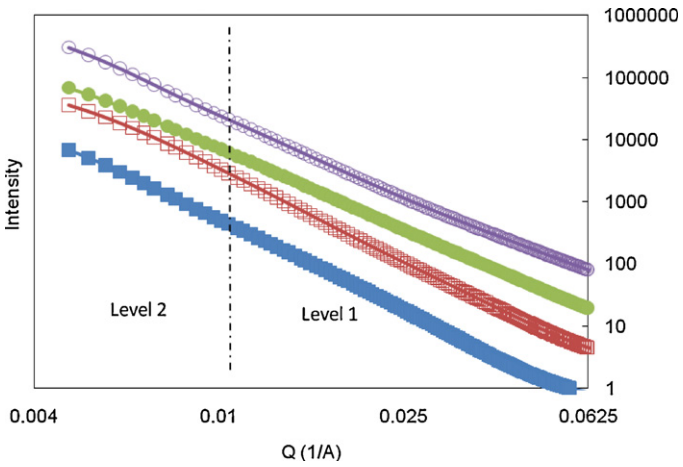

Fig. 4. The unified fit of SAXS profile of photoperiod-sensitive sorghum with different pretreatments ((■) untreated; (□) acid treated; (●) alkali treated; (○) ammonia treated). The curves were shifted vertically for better visualization.

cellulose pore closure (McMillan, 1994), which might be another reason for the shape change.

After the 1D intensity profile was obtained by integrating the 2D pattern (see supporting information), curve features were analyzed using a model fitting procedure. A unified model, which contains a Guinier region and a power-law region, was successfully employed to fit the intensity data with different levels (Fig. 4). The related parameters were compared in Table 3. In level 1, a length scale of about 100–600 Å, the R_g decreased significantly after the pretreatments. The particles in this length scale showed the characteristic of a surface fractal.

In level 2, a length scale ranging from 600 to 1400 Å, both treated and untreated samples showed downward curves that could be used to calculate the R_g of particles (Table 3). The level at length scale from 1000 Å was considered to correspond to cellulose structure (Pingali et al., 2010b). In this case, the results showed that the radius of cellulose aggregates decreased from 481.6 Å with various pretreatments. The R_g of the acid treated sample was significantly reduced to 418.7 Å. It is well known that the glycosidic linkage of cellulose is susceptible to acid-catalyzed hydrolysis (Chang, Pound, & Manley, 1973), and cellulose is easily degraded during acid pretreatment at a high temperature (Mosier, Hendrickson, et al., 2005; Mosier, Wyman, et al., 2005). The results from WAXD also suggested that both crystalline and amorphous cellulose were degraded during the acid pretreatment. Thus, the significantly reduced R_g could be a result of cellulose degradation. After the acid pretreatment, the cellulose structure displayed the characteristic of surface fractal with a surface fractal dimension (d_s) of 2.02, reflecting a smooth pore-boundary surface (Bale & Schmidt, 1984; Pingali et al., 2010b).

The structural changes of cellulose with acid pretreatment are complicated and dependent on pretreatment conditions and probably on the type of biomass. In this study, the crystalline structure of cellulose was distorted as the orientation factor decreased (Table 2), and part of the crystalline cellulose was degraded. It is not conclusive yet that the structural changes of cellulose are favorable cellulase digestion. A previous study using biomass powder suggested a decrease in cellulose crystallinity after acid pretreatment (Xu et al., 2011), but a recent study of pure cellulose showed different results and suggested that sulfuric acid increased cellulose crystallinity because amorphous cellulose was hydrolyzed preferentially by acid (Zhao et al., 2006). The discrepancy could be due to the differences in processing conditions and in the complicated 3D structure of biomass. Bonds in the amorphous regions of cellulose are initially susceptible to acid hydrolysis but the fragments released during hydrolysis could associate into crystalline form (Bertran & Dale, 1985; Wadehra & Manley, 1965). Thus, cellulose crystallinity, which is related to the initial rate and the overall conversion efficiency of enzymatic hydrolysis (Bertran & Dale, 1985; Fan, Lee, & Beardmore, 1980), changes depending on biomass structure and pretreatment conditions.

Notably, for the changes of the network structure of biomass with the acid pretreatment, significant removal of hemicellulose, as well as the structural disruption of lignin, would have positive effects on the efficiency of enzymatic hydrolysis. For example, lignin disruption reduced lignin-cellulase absorption (Mansfield, Mooney, & Saddler, 1999). Therefore, acid pretreatment is effective for increasing the conversion efficiency of enzymatic hydrolysis by disrupting biomass structure, but if the crystallinity of cellulose increases after acid hydrolysis, it is not conclusive that acid pretreatment is effective for making the cellulose itself in the solid form of biomass more susceptible to enzymatic hydrolysis.

Also notable is the effect of the drying process on structure, which is not negligible, although both dry cellulose and water-saturated cellulose were found to contain hydrophobic microregions (Grigoriew, Chmielewski, & Amenitsch, 2001). SAXS study on fiber also suggested that microvoids changed significantlyduring drying and rewetting (Vickers et al., 2001). The removal of the amorphous part, especially delignification, will significantly decrease the density of mass structure and possibly result in structure collapse with drying (Teleman, Larsson, & Iversen, 2001). Thus, in situ study of structural change during pretreatment is suggested.

Table 3
SAXS results with unified model.[a,b]

	Level 1		Level 2		
	R_g (Å)	P	R_g (Å)	P	d_s
Untreated	100.8 ± 4.8	2.93	481.6 ± 2.0	3.57	2.43
Acid treated	62.4 ± 0.8	3.41	418.2 ± 0.9	3.98	2.02
Alkali treated	46.5 ± 0.7	3.17	436.9 ± 1.2	3.30	2.70
Ammonia treated	43.4 ± 0.9	3.17	460.2 ± 0.9	3.37	2.63

[a] R_g is radius of gyration. P is power-law exponent. d_s is surface fractal dimension.
[b] Errors reported were propagated from the counting error in the raw data.

4. Conclusions

For the first time, the structure of different parts of PS sorghum and structural changes during pretreatments were studied by both WAXD and SAXS. Using a combination of WAXD and SAXS revealed the structure of lignocellulosic biomass, including multiple components in both crystalline and amorphous states. Using biomass chips made it possible to reveal crystal orientation distribution changes and their effects on biomass processing. Hence, strategic design of biofuel production could be guided by the structural information at a molecular level.

Fundamentally understanding the structural discrepancies among different parts of biomass is important for utilizing biomass efficiently to reduce processing cost. WAXD study shows that the structure of cellulose in the outside rind has crystal orientation with a parameter of 0.26, whereas the structure of cellulose in other parts is isotropic. Future study should be conducted on the effects of crystal orientation on biomass processing: such efforts could be helpful for biomass breeding, screening, and process design. WAXD results also show that the PS sorghum rind has the highest crystallinity, and the isotropic structure of the leaf is less ordered. Meanwhile, SAXS study suggested that all biomass samples are surface fractals. Needle-shaped microvoids were found in the rind.

Design of pretreatment process has never obtained so much attention. Although many pretreatment studies are reported, the

intrinsic mechanism of biomass structural change during pretreatment is not clear yet. With the acid pretreatment, cellulose structure was changed as indicated by a decrease of orientation factor and partial degradation of crystalline cellulose. A smooth pore-boundary structure of cellulose was suggested by the SAXS results. With the alkali pretreatment, cellulose structure was modified with an increased orientation factor and an increased crystal size, and metastable cellulose I was transformed partially to stable cellulose II.

Acknowledgments

We thank Dr. Dufei Fang and Dr. Jan Ilavsky for their help with data processing, and Drs. Jun Wang, Benjamin S. Hsiao, and Lixia Rong for their assistance in WAXD and SAXS studies. Use of the National Synchrotron Light Source, Brookhaven National Laboratory, was supported by the U.S. Department of Energy, Office of Science, Office of Basic Energy Sciences, under Contract No. DE-AC02-98CH10886. The study was supported in part by the Center for Sustainable Energy, Kansas State University. This is contribution number 11-290-J from the Kansas Agricultural Experiment Station.

References

Alagarswamy, G., Reddy, D., & Swaminathan, G. (1998). Durations of the photoperiod-sensitive and-insensitive phases of time to panicle initiation in sorghum. *Field Crops Research*, *55*(1-2), 1–10.

Alexander, L. (1954). The synthesis of X-ray Spectrometer line profiles with application to crystallite size measurements. *Journal of Applied Physics*, *25*, 155.

Aravindanath, S., Iyer, P., & Sreenivasan, S. (1986). Communications to the editor, Further evidence for the presence of cellulose I and II in the same cross section of partially mercerized cotton fibers. *Textile Research Journal*, *56*(3), 211–212.

Astley, O., & Donald, A. (2001). A small-angle X-ray scattering study of the effect of hydration on the microstructure of flax fibers. *Biomacromolecules*, *2*(3), 672–680.

Balan, V., da Costa Sousa, L., Chundawat, S., Marshall, D., Sharma, L., Chambliss, C., & Dale, B. (2009). Enzymatic digestibility and pretreatment degradation products of AFEX-treated hardwoods (*Populus nigra*). *Biotechnology Progress*, *25*(2), 365–375.

Bale, H., & Schmidt, P. (1984). Small-angle X-ray-scattering investigation of submicroscopic porosity with fractal properties. *Physical Review Letters*, *53*(6), 596–599.

Beaucage, G. (1995). Approximations leading to a unified exponential/power-law approach to small-angle scattering. *Journal Applied Crystallographica*, *28*(6), 717–728.

Berlin, A., Gilkes, N., Kurabi, A., Bura, R., Tu, M., Kilburn, D., & Saddler, J. (2005). Weak lignin-binding enzymes. *Applied Biochemistry and Biotechnology*, *121*(1), 163–170.

Bertran, M., & Dale, B. (1985). Enzymatic hydrolysis and recrystallization behavior of initially amorphous cellulose. *Biotechnology and Bioengineering*, *27*(2), 177–181.

Blazek, J., & Gilbert, E. P. (2011). Application of small-angle X-ray and neutron scattering techniques to the characterisation of starch structure: A review. *Carbohydrate Polymer*, *85*(2), 281–293.

Britton, T., Liang, H., Dunne, F., & Wilkinson, A. (2010). The effect of crystal orientation on the indentation response of commercially pure titanium: Experiments and simulations. *Proceedings of the Royal Society A: Mathematical, Physical and Engineering Science*, *466*(2115), 695.

Burger, C., Hsiao, B. S., & Chu, B. (2010). Preferred orientation in polymer fiber scattering. *Polymer Reviews*, *50*(1), 91–111.

Canetti, M., Bertini, F., De Chirico, A., & Audisio, G. (2006). Thermal degradation behaviour of isotactic polypropylene blended with lignin. *Polymer Degradation and Stability*, *91*(3), 494–498.

Chang, M., Pound, T., & Manley, R. (1973). Gel-permeation chromatographic studies of cellulose degradation I. Treatment with hydrochloric acid. *Journal of Polymer Science: Polymer Physics Edition*, *11*(3), 399–411.

Chen, X., Burger, C., Fang, D., Ruan, D., Zhang, L., Hsiao, B., & Chu, B. (2006). X-ray studies of regenerated cellulose fibers wet spun from cotton linter pulp in NaOH/thiourea aqueous solutions. *Polymer*, *47*(8), 2839–2848.

Chen, X., Burger, C., Wan, F., Zhang, J., Rong, L., Hsiao, B., Chu, B., Cai, J., & Zhang, L. (2007). Structure study of cellulose fibers wet-spun from environmentally friendly NaOH/urea aqueous solutions. *Biomacromolecules*, *8*(6), 1918–1926.

Chu, B., & Hsiao, B. (2001). Small-angle x-ray scattering of polymers. *Chemical Reviews*, *101*(6), 1727–1762.

Clerget, B., Dingkuhn, M., Goze, E., Rattunde, H., & Ney, B. (2008). Variability of phyllochron, plastochron and rate of increase in height in photoperiod-sensitive sorghum varieties. *Annals of Botany*, *101*(4), 579–594.

Crawshaw, J., Bras, W., Mant, G., & Cameron, R. (2002). Simultaneous SAXS and WAXS investigations of changes in native cellulose fiber microstructure on swelling in aqueous sodium hydroxide. *Journal of Applied Polymer Science*, *83*(6), 1209–1218.

Fan, L., Lee, Y., & Beardmore, D. (1980). Mechanism of the enzymatic hydrolysis of cellulose: effects of major structural features of cellulose on enzymatic hydrolysis. *Biotechnology and Bioengineering*, *22*(1), 177–199.

Gancy, A. (1963). Thermal Decomposition of Sodium Sesquicarbonate. *Journal of Chemical Engineering Data*, *8*(3), 301–306.

Gardner, K., & Blackwell, J. (1974). The structure of native cellulose. *Biopolymers*, *13*(10), 1975–2001.

Gassan, J., & Bledzki, A. (1999). Alkali treatment of jute fibers: Relationship between structure and mechanical properties. *Journal of Applied Polymer Science*, *71*(4), 623–629.

Grigoriew, H., Chmielewski, A., & Amenitsch, H. (2001). Structural temperature transformation of the cellulose-water system using time-resolved SAXS. *Polymer*, *42*(1), 103–108.

Gurarie, V. N., Otsuka, P. H., Jamieson, D. N., Williams, J. S., & Conway, M. (2002). The effect of crystal orientation on thermal shock-induced fracture and properties of ion implanted sapphire. *Nuclear Instruments and Methods in Physics Research Section B: Beam Interactions with Materials and Atoms*, *190*(1–4), 751–755.

Heiner, A., & Teleman, O. (1997). Interface between monoclinic crystalline cellulose and water: breakdown of the odd/even duplicity. *Langmuir*, *13*(3), 511–518.

Hermans, P., Vermaas, D., & Weidinger, A. (1950). Recrystallization of regenerated cellulose upon mercerization. *Nature*, *165*, 238.

Hidaka, H., Takizawa, T., Fujikawa, H., Ohneda, T., & Fukuzumi, T. (1984). A study on the inhibition of cellulolytic activities by lignin. *Applied Biochemistry and Biotechnology*, *9*(4), 367.

Jakob, H., Fengel, D., Tschegg, S., & Fratzl, P. (1995). The elementary cellulose fibril in Picea abies: Comparison of transmission electron microscopy, small-angle X-ray scattering, and wide-angle X-ray scattering results. *Macromolecules*, *28*(26), 8782–8787.

Jakob, H., Fratzl, P., & Tschegg, S. (1994). Size and arrangement of elementary cellulose fibrils in wood cells: A small-angle X-ray scattering study of Picea abies. *Journal of Structural Biology*, *113*(1), 13–22.

Jungnikl, K., Paris, O., Fratzl, P., & Burgert, I. (2008). The implication of chemical extraction treatments on the cell wall nanostructure of softwood. *Cellulose*, *15*(3), 407–418.

Koberstein, J., Morra, B., & Stein, R. (1980). The determination of diffuse-boundary thicknesses of polymers by small-angle X-ray scattering. *Journal of Applied Crystallography*, *13*(1), 34–45.

Kolpak, F., & Blackwell, J. (1976). Determination of the structure of cellulose II. *Macromolecules*, *9*(2), 273–278.

Konnerth, J., Gierlinger, N., Keckes, J., & Gindl, W. (2009). Actual versus apparent within cell wall variability of nanoindentation results from wood cell walls related to cellulose microfibril angle. *Journal of Materials Science*, *44*(16), 4399–4406.

Kroon-Batenburg, L., Bouma, B., & Kroon, J. (1996). Stability of cellulose structures studied by MD simulations. Could mercerized cellulose II Be parallel? *Macromolecules*, *29*(17), 5695–5699.

Lichtenegger, H., Reiterer, A., Stanzl-Tschegg, S., & Fratzl, P. (1999). Variation of cellulose microfibril angles in softwoods and hardwoods—a possible strategy of mechanical optimization. *Journal of Structural Biology*, *128*(3), 257–269.

Mansfield, S. D., Mooney, C., & Saddler, J. N. (1999). Substrate and enzyme characteristics that limit cellulose hydrolysis. *Biotechnology Progress*, *15*(5), 804–816.

McMillan, J. (1994). Pretreatment of lignocellulosic biomass. In J. O. B. Michael, E. Himmel, & R. P. Overend (Eds.), *Enzymatic Conversion of Biomass for Fuels Production* (pp. 292–324). Washington: ACS Publications.

Mielenz, J. (2001). Ethanol production from biomass: technology and commercialization status. *Current Opinion in Microbiology*, *4*(3), 324–329.

Mosier, N., Hendrickson, R., Ho, N., Sedlak, M., & Ladisch, M. (2005). Optimization of pH controlled liquid hot water pretreatment of corn stover. *Bioresource Technology*, *96*(18), 1986–1993.

Mosier, N., Wyman, C., Dale, B., Elander, R., Lee, Y., Holtzapple, M., & Ladisch, M. (2005). Features of promising technologies for pretreatment of lignocellulosic biomass. *Bioresource Technology*, *96*(6), 673–686.

Nishiyama, Y., Kim, U. J., Kim, D. Y., Katsumata, K. S., Roland, P., & Langan, P. (2003). Periodic disorder along ramie cellulose microfibrils. *Biomacromolecules*, *4*(4), 1013–1017.

Nishiyama, Y., Langan, P., & Chanzy, H. (2002). Crystal structure and hydrogen-bonding system in cellulose Iβ from synchrotron X-ray and neutron fiber diffraction. *Journal of the American Chemical Society*, *124*(31), 9074–9082.

Oh, S., Yoo, D., Shin, Y., Kim, H., Kim, H., Chung, Y., Park, W., & Youk, J. (2005). Crystalline structure analysis of cellulose treated with sodium hydroxide and carbon dioxide by means of X-ray diffraction and FTIR spectroscopy. *Carbohydrate Research*, *340*(15), 2376–2391.

Pingali, S. V., Urban, V. S., Heller, W. T., McGaughey, J., O'Neill, H. M., Foston, M., Myles, D. A., Ragauskas, A. J., & Evans, B. R. (2010). SANS study of cellulose extracted from switchgrass. *Acta Crystallographica Section D: Biological Crystallography*, *66*(11), 1189–1193.

Pingali, S. V., Urban, V. S., Heller, W. T., McGaughey, J., O'Neill, H., Foston, M., Myles, D. A., Ragauskas, A., & Evans, B. R. (2010). Breakdown of cell wall nanostructure in dilute acid pretreated biomass. *Biomacromolecules*, *11*(9), 2329–2335.

Ran, S., Wang, Z., Burger, C., Chu, B., & Hsiao, B. (2002). Mesophase as the precursor for strain-induced crystallization in amorphous poly (ethylene terephthalate) film. *Macromolecules*, *35*(27), 10102–10107.

Rondeau-Mouro, C., Bouchet, B., Pontoire, B., Robert, P., Mazoyer, J., & Buléon, A. (2003). Structural features and potential texturising properties of lemon and maize cellulose microfibrils. *Carbohydrate Polymer*, *53*(3), 241–252.

Rosenow, D., Quisenberry, J., Wendt, C., & Clark, L. (1983). Drought tolerant sorghum and cotton germplasm. *Agricultural Water Management*, *7*(1–3), 207–222.
Roy, C., Budtova, T., & Navard, P. (2003). Rheological properties and gelation of aqueous cellulose–NaOH solutions. *Biomacromolecules*, *4*(2), 259–264.
Rubin, E. (2008). Genomics of cellulosic biofuels. *Nature*, *454*(7206), 841–845.
Schmidt, P. (1991). Small-angle scattering studies of disordered, porous and fractal systems. *Journal of Applied Crystallography*, *24*(5), 414–435.
Silverstein, R. A., Chen, Y., Sharma-Shivappa, R. R., Boyette, M. D., & Osborne, J. (2007). A comparison of chemical pretreatment methods for improving saccharification of cotton stalks. *Bioresource Technology*, *98*(16), 3000–3011.
Teleman, A., Larsson, P., & Iversen, T. (2001). On the accessibility and structure of xylan in birch kraft pulp. *Cellulose*, *8*(3), 209–215.
Vickers, M., Briggs, N., Ibbett, R., Payne, J., & Smith, S. (2001). Small angle X-ray scattering studies on lyocell cellulosic fibres: the effects of drying, re-wetting and changing coagulation temperature. *Polymer*, *42*(19), 8241–8248.
Wadehra, I., & Manley, R. (1965). Recrystallization of amorphous cellulose. *Journal of Applied Polymer Science*, *9*(7), 2627–2630.
Xu, F., Shi, Y.-C., Wu, X., Theerarattananoon, K., Staggenborg, S., & Wang, D. (2011). Sulfuric acid pretreatment and enzymatic hydrolysis of photoperiod sensitive sorghum for ethanol production. *Bioprocess and Biosystems Engineering*, *34*(4), 485–492.
Yu, P., McKinnon, J., Christensen, C., Christensen, D., Marinkovic, N., & Miller, L. (2003). Chemical imaging of microstructures of plant tissues within cellular dimension using synchrotron infrared microspectroscopy. *Journal of Agricultural and Food Chemistry*, *51*(20), 6062–6067.
Zhao, H., Kwak, J. H., Wang, Y., Franz, J. A., White, J. M., & Holladay, J. E. (2006). Effects of crystallinity on dilute acid hydrolysis of cellulose by cellulose ball-milling study. *Energy and Fuels*, *20*(2), 807–811.